HHS Public Access

COG complexes form spatial landmarks for distinct SNARE complexes

Rose Willett[*,§], **Tetyana Kudlyk**[*,§], **Irina Pokrovskaya**[*], **Robert Schönherr**[‡], **Daniel Ungar**[†], **Rainer Duden**[‡], and **Vladimir Lupashin**[*]

[*]Department of Physiology and Biophysics, UAMS, Little Rock, AR

[†]University of York, Department of Biology, York, UK

[‡]Institute of Biology, Center of Structural and Cell Biology in Medicine, University of Lübeck, Germany

Abstract

Vesicular tethers and SNAREs are two key protein components of the intracellular membrane trafficking machinery. The COG (conserved oligomeric Golgi) complex has been implicated in the tethering of retrograde intra-Golgi vesicles. Here, using yeast two hybrid and co-immunoprecipitation approaches, we show that three COG subunits, namely COG4, 6, and 8, are capable of interacting with defined Golgi SNAREs, namely STX5, STX6, STX16, GS27, and SNAP29. Comparative analysis of COG8-STX16 and COG4-STX5 interactions by a COG-based mitochondrial re-localization assay reveals that the COG8 and COG4 proteins initiate the formation of two different tethering platforms that can facilitate the redirection of two populations of Golgi transport intermediates to the mitochondrial vicinity. Our results uncover a role for COG subcomplexes in defining the specificity of vesicular sorting within the Golgi.

The transport of vesicular carriers in the secretory pathway is a multistep process that includes vesicle budding, tethering, docking, and fusion[1]. Vesicle tethering, the initial contact between an intracellular trafficking vesicle and its membrane target, requires the participation of both long coiled-coil tethers and multi-subunit hetero-oligomeric tethering complexes (MTCs)[2]. Tethering complexes, in concert with small Rab GTPases, Sec1/Munc18(SM) proteins, and SNAREs, regulate the docking of a vesicle to its acceptor

Corresponding author: Dr. Vladimir Lupashin, Department of Physiology and Biophysics, University of Arkansas for Medical Sciences, Biomed 261-2, Mail slot 505, 4301 West Markham Street, Little Rock, AR 72205, USA. tel 501-603-1170 ; fax 501-686-8167, vvlupashin@uams.edu.
§equal contribution

Contributing authors: Dr. Daniel Ungar, Department of Biology (Area 9), University of York, Wentworth Way, Heslington, York,YO10 5DD, UK, Dr. Rainer Duden, Center for Structural and Cell Biology in Medicine, Institute of Biology, University of Luebeck, Ratzeburger Allee 160, 23562 Luebeck, Germany

Author contributions
Experiments were designed by R.W., T.K., D.U., R.D. and V.L.; T.K. performed yeast two-hybrid screen; R.W. and T.K. performed co-IP and IF analysis; I.P. performed electron microscopy; R.S. performed live-cell microscopy and cell fusion assay. R.W., D.U., R.D. and V.L. prepared the manuscript.

Conflict of interest statement
None declared.

compartment, and thereby determine the targeting specificity of vesicles. Such targeting is a critical determinant of protein sorting, and thus maintaining the compartmental identity within the secretory pathway.

MTCs form a group of large evolutionary conserved peripheral protein complexes that function throughout the secretory pathway. Included within this superfamily of proteins is a family termed CATCHR (complexes associated with tethering containing helical rods) that consist of the Conserved Oligomeric Golgi (COG) complex, the Golgi-associated retrograde protein (GARP) complex, the Exocyst complex, and the Dsl1 complex[3]. Multiple modes of interaction between MTCs and other components of the vesicle docking/fusion machinery have recently been suggested[4–7].

The COG complex consists of eight subunits named COG1–8[8, 9], grouped into two subcomplexes: COG1–4 (Lobe A) and COG5–8 (Lobe B)[10, 11]. The COG complex functions in the tethering of vesicles recycling resident Golgi proteins (such as glycosylation enzymes)[12]. Consequently, defects in COG complex subunits result in congenital disorders of glycosylation (CDG) type II[13]. We have shown previously that the yeast and mammalian COG complex interacts with the Sed5/STX5 containing SNARE complex[14, 15] through a direct interaction between COG4 and Sed5/STX5. Interference with this interaction results in a decreased steady state level of intra-Golgi SNARE complexes.

In this study, we have extended our initial investigation of COG-SNARE interactions to include 14 known Golgi-localized SNARE proteins and all COG subunits. Our results demonstrate specific interactions of COG4, 6, and 8 with the five Golgi SNAREs STX5, STX6, STX16, GS27, and SNAP29 by yeast two hybrid and native co-immunoprecipitation approaches. A mitochondrial COG relocalization assay revealed a unique feature of COG-SNARE interactions, with COG4 mislocalization redirecting STX5-containing vesicles, and COG8 mislocalization redirecting STX16-containing membranes to COG-occupied mitochondria. Our results indicate that one of the major functions of COG sub-complexes is to serve as landmarks for the initiation of tethering platforms for at least two different types of intra-Golgi vesicles.

Results

COG complex interacts with multiple Golgi SNAREs

To uncover the complete set of COG-SNARE interactions we performed a directed yeast two hybrid screen of all 8 COG subunits with 14 Golgi localized SNARE proteins. Of these only the Qa SNAREs STX5 and STX16, the Qb SNARE GS27, the Qc SNARE STX6, and the Qab SNARE SNAP29 displayed positive interactions with subunits of the COG complex (Table 1, and Supplementary Figure S1). Similarly, only a subset of the COG subunits, namely COG4, 6 and 8, displayed an interaction with SNAREs. As previously reported[15], COG4 demonstrated a unique interaction with STX5 under strong selection (−Ade). COG6, in addition to previously reported interactions with STX5[15] and STX6[16], also specifically interacted with GS27 and SNAP29. Finally, COG8 displayed a novel set of interactions with the SNAREs STX5, STX6, STX16, and GS27, of these STX5, STX16, and GS27 were observed under stringent selection conditions (Table 1, and Supplementary Figure S1). The

observed yeast two hybrid interactions were validated in co-immunoprecipitation (co-IP) experiments (Supplementary Figure S2).

To further characterize the novel interaction between COG8 and STX16, we constructed truncated mutants of both COG8-myc (based on predicted breaks in the alpha-helical domains) and GFP-STX16 (at known domain boundaries) (Figure 1a), and tested them for interaction by co-IP. COG8-myc 8–184 was immunoprecipitated as efficiently by GFP-STX16 as full length COG8-myc, indicating that the COG8 N-terminal domain is dispensable for the COG8-STX16 interaction. Significant co-IP (4%) was also observed for the STX16-COG8-myc 8–436 pair, indicating that the C terminal domain of COG8 is partially sufficient for the interaction with STX16 (Figure 1b, lanes 1–3). Furthermore, truncated mutants of GFP-STX16 reveal that both the N-terminal (aa 2–73) and the Habc (aa 73–169) domains of STX16 are dispensable for the COG8-STX16 interaction, indicating that the C-terminal SNARE domain-containing region of STX16 is the major binding partner of COG8 (Figure 1b, lanes 4–6).

COG targeting to mitochondria causes relocalization of Golgi markers

To gain a better understanding of the nature and hierarchy of COG-SNARE interactions, a mitochondrial mislocalization strategy[17] was employed. siRNA-resistant COG complex subunits were fused to mCherry fluorescent protein and the mitochondrial-targeting ActA sequence from *Listeria* (Figure 2a). Transient expression of mCherry-ActA (mChActA) demonstrated intense labeling of the mitochondrial network without any visible effect on Golgi or mitochondrial structure (Figure 2b). Surprisingly, expression of either COG8-mChActa (Figure 2c, d) or COG4-mChActA (Figure 2e, g) caused dramatic changes to both Golgi and mitochondrial morphology. Both immunofluorescence (IF) (Figure 2b–e) and EM (Figure 2f–g) approaches revealed that in cells expressing either COG8-mChActa or COG4-mChActA the majority of the mitochondria were aggregated while Golgi membranes were severely fragmented (Figure 2l). Importantly, aggregation of the mitochondria was not the result of possible crosslinking via COG8 or COG4 self-dimerization, since these subunits did not show any potency for self-dimerization in either yeast two hybrid or mammalian expression assays[11]. Overexpression of COG4-myc partially alleviated the COG4-mChActA-induced mitochondrial aggregation (Supplementary Figure S3), possibly by competing for the additional proteins and/or membranes responsible for this aggregation.

Next we used a gene replacement strategy to test the localization of Golgi Qa SNAREs in cells that carry only the mitochondria-localized COG subunits. STX16 demonstrated a punctate localization in COG8-deficient cells, and these STX16-positive vesicles were concentrated in the vicinity of COG8-mChActA aggregated mitochondria (Figure 2h, arrow). This pattern was specific for STX16 (and distinct from its WT localization (Supplementary Figure S4a)) since endogenous STX5 was mostly excluded from the area occupied by COG8-mChActA-positive mitochondria (Figure 2i). In dramatic contrast, STX5 showed significant co-localization with the COG4-mChActA signal (Figure 2j, arrow) while STX16 was mostly excluded from the vicinity of COG4-mChActA aggregated mitochondria (Figure 2k). Since both STX5 and STX16 are transmembrane proteins their co-localization with COG-decorated mitochondria indicates the relocalization of SNARE-containing

vesicles to the mitochondria vicinity. In summary, gene replacement/relocalization experiments revealed that localization of the endogenous STX16-containing membranes is sensitive to the location of COG8, while STX5 ones are sensitive to the intracellular location of COG4.

Expression of COG6-mChActA resulted in some mitochondrial aggregation but did not affect either Golgi morphology or localization of Golgi SNARE proteins, and therefore COG6-mChActA was investigated separately[18].

In order to accurately quantify the COG4-mChActA induced relocalization of STX5-containing vesicles to mitochondria, we transiently expressed fluorescently tagged STX5 in HeLa cells. Line plot analysis and Pearsons correlation coefficient demonstrated extensive co-localization of GFP-STX5-containing vesicles with COG4 labeled mitochondria (Figure 3b, g), validating our results seen with the endogenous protein. In contrast, GFP-STX16 membranes did not move toward COG4-mChActA-populated mitochondria (Figure 3d, g), indicating that the relocalization of GFP-STX5 vesicles was specific for COG4. Some relocalization to the mitochondria was observed for the STX5 intra-Golgi partner SNARE proteins GS28 and GS27 (Figure 3g, and Supplementary Figure S5a, b), while the ER-Golgi SNAREs Bet1 and Sec22 were negative for co-localization to COG4 labeled mitochondria (Figure 3g and Supplementary Figure S5c, d). Similarly, COG4-dependent relocalization of STX5 vesicles to mitochondria was observed in cells that stably express GFP-STX5 on the Golgi (Supplementary Figure S6) and in cell fusion experiments (Supplementary Figures S7, S8), indicating that de-novo synthesis of Golgi SNARE molecules is dispensable for their relocalization, and that STX5-containing vesicles are re-routed to the mitochondria vicinity directly from the Golgi region.

COG4 interacts physically not only with STX5, but also with its partner protein Sly1[19]. Interestingly, the COG4(E53A, E71A)- mChActA double mutant, which does not interact with Sly1p, was not capable of attracting GFP-STX5 vesicles (Supplementary Figure S9), indicating that the functional STX5-Sly1 complex is essential for the movement and/or tethering of STX5 vesicles to COG4-mitochondria.

To test if displacement of COG4 to the mitochondria would influence the localization of other COG subunits, we transfected COG4-mChActA into cell lines stably expressing YFP-COG3 (Figure 3e, g) or GFP-COG6 (Figure 3f, g). Both YFP-COG3 and GFP-COG6 became significantly colocalized with COG4-mChActA-labeled mitochondria. Similar results were obtained with both myc-COG2 and COG8-GFP (Supplementary Figure S10), indicating that the entire COG complex relocalized to the COG4 decorated mitochondria. Native immunoprecipitation experiments confirmed that a significant fraction of both myc-COG2 (Lobe A subunit) and COG6-myc (Lobe B subunit) was specifically recovered in COG4mChActA IP (Supplementary Figure S11), indicating that the entire COG complex is assembled on the mitochondrial membrane. This relocalization was specific for COG subunits since the *cis*-Golgi resident proteins p115 (Figure 3b, e) and Giantin (Figure 3d, f) remained associated with fragmented Golgi membranes.

Disrupting the interaction of lobes A and B, either by overexpressing a C-terminal fragment of COG1, or by knocking down the COG1 subunit (Supplementary Figure S12), significantly diminished the relocalization of GFP-STX5 to the COG4-populated mitochondrial membranes, suggesting that the assembly of the functional COG complex on mitochondria is essential for relocalization of STX5-bearing vesicles.

Our protein-protein interaction data (Table 1 and Supplementary Figure S1) indicated that STX5 can bind the COG8 protein to the same or even greater extent as COG4; therefore we expected that GFP-STX5-bearing vesicles would be re-localized to COG8-decorated mitochondria. To our surprise, in cells that express COG8-mChActA, GFP-STX5 mostly localized to perinuclear fragmented Golgi membranes (Figure 4b, g), indicating that COG8 alone is not sufficient to attract STX5-containing trafficking intermediates. In contrast, the GFP-STX16 signal was significantly co-localized with COG8-mChActA-decorated mitochondria (Figure 4c, g), indicating that the STX16-bearing trafficking intermediates become re-routed from the Golgi to another cellular location (presumably to the organelle possessing the highest concentration of COG8 protein). Rapid relocalization of STX16 vesicles to mitochondria was observed in cell fusion experiments (Supplementary Figure S13), indicating that de-novo synthesis of this Golgi SNARE molecule is dispensable for its relocalization and that STX16-containing vesicles were re-routed to mitochondria directly from the trans-Golgi region and/or endosomal compartment.

Co-expression of COG8-mChActA and YFP-COG3 (Figure 4e, g) revealed that YFP-COG3 did not relocalize to mitochondria, indicating that the Lobe A subunits of COG did not follow COG8. In contrast, GFP-COG6 (Figure 4f, g) was faithfully recruited to COG8-occupied mitochondria. Since COG6 interacts with COG8 only in the presence of other Lobe B subunits[11], our results suggest that Lobe B, in its entirety, assembles onto outer mitochondrial membranes decorated with COG8-mChActA. In agreement with this, native immunoprecipitation experiments confirmed that COG6-myc was specifically recovered in a COG8mChActA IP, while myc-COG2 recovery was at background level (Supplementary Figure S11), indicating that Lobe A subunits are excluded from COG8-decorated mitochondrial membranes. This result is in a good agreement with both previously published, and our recent unpublished data, indicating that approximately 10% of cytoplasmic[9] and 40% of membrane-bound Lobe B exists as the Lobe A-independent sub-complex (Willett, Lupashin; in preparation).

As demonstrated above, STX16 is a major SNARE partner of COG8; therefore we reasoned that direct protein-protein interactions could be the major driving force behind the GFP-STX16 relocalization to mitochondria. To examine this possibility, two truncated mutants of COG8 were tested for their ability to redirect trafficking of GFP-STX16-containing vesicles to mitochondria. Both truncated mutants were capable of binding STX16, as demonstrated by native co-IP (Figure 1b), but failed to redirect STX16 transport intermediates to mitochondria (Figure 4g) suggesting that the direct COG8-STX16 protein-protein interaction is not sufficient to attract STX16-containing vesicles to a new cellular location. Similarly, two truncated mutants of STX16 were not diverted to the COG8-populated mitochondria (Figure 4g), suggesting that only vesicles bearing functional (full-length) STX16 are capable of following fully active COG8 to mitochondrial membranes. The

STX16 relocalization appeared to be independent from Lobe A of the COG complex; interaction of STX16 membranes with COG8-mitochondria was not disturbed in cells depleted of COG2 and COG3 proteins (Figure 4g). Endogenous COG8 was also dispensable for the relocalization of STX16 vesicles to COG8-mChActA-populated mitochondria (Figure 4g).

Finally we found that redirection of STX16 vesicles to mitochondria was severely disturbed in cells that over-express the STX16 partner protein Vps45 (Figure 4g). This suggests that movement of STX16 vesicles to mitochondria recapitulates a *bona fide* membrane transport step, with COG8 serving as a specific spatial landmark for these STX16 trafficking intermediates.

To further investigate the nature of the interaction between COG8-populated mitochondria and STX16 trafficking intermediates, we performed a FRAP assay with cells that co-express COG8-mChActA and GFP-STX16 (Figure 5). We found that recovery of GFP-STX16 signal in a bleached area was relatively fast in comparison to the recovery of the mCherry signal, showing that STX16 vesicles are rapidly exchanging on COG8-mitochondria. This indicates that the Lobe B tethering machinery alone is not sufficient for the tight docking of STX16 transport carriers. Furthermore, these results may also indicate that tethering interactions are transient, and that there is a built-in timer that aborts tethering if fusion does not follow.

Transmission electron microscopy (TEM) was employed for a detailed analysis of STX5 and STX16-containing trafficking intermediates that move to mitochondrial membranes in response to relocalization of COG subunits. Low resolution TEM images (Figure 2f, g) confirmed that in cells expressing high levels of COG4-mChActA the mitochondria were mostly found in aggregates. At higher magnification both membrane tubules and multiple vesicle profiles (arrows) were observed in close proximity to COG4-mChActA (Figure 6a) and COG8-mChActA (Figure 6b) populated mitochondria. Vesicles adjacent to mitochondria were uniform in size (60–80nm), and often connected to the outer mitochondrial membranes by string-like structures (Supplementary Figure S14) that likely represent protein tethers such as the COG complex and/or COG-associated proteins. Similar fibrous elements which link vesicle profiles to larger membranes were described previously for vesicles tethered to Golgi cisternae[20]. Immuno-EM with anti-GFP antibodies confirmed that vesicles located in close proximity to (and often in-between) mitochondria were carrying GFP-STX5 (Figure 6c) and GFP-STX16 (Figure 6d). In contrast, in cells that expressed mChActA and GFP-tagged SNAREs, the GFP signal was mostly localized to the Golgi (Figure 6e, f).

COG8-mChActA misdirects Shiga Toxin transporting vesicles to mitochondria

We, and others, demonstrated previously that both the COG complex[16, 21] and STX16[22] are essential for the intracellular delivery of Shiga Toxin from the endosomal compartment to the Golgi. To test if redirection of STX16 vesicles to the COG8-populated mitochondria affects the delivery of Shiga toxin, cells co-expressing COG8-mChActA and GFP-STX16 were pulsed with fluorescent Shiga toxin B subunit (STB-647), and then chased for 2 hours in fresh media. In COG8-mChActA expressing cells, the majority of GFP-STX16 and

STB-647 were accumulated in close proximity to mitochondria, suggesting that endosome-to-Golgi trafficking intermediates that carry STB-647 and GFP-STX16 are redirected to the COG8-mChActA-populated mitochondrial membranes (Figure 7a). In control cells co-expressing mChActA and GFP-STX16, the majority of STB-647 was found in the perinuclear area (Figure 7b), confirming the role of COG8 in determining the fate of STB-647-containing TGN vesicles. Accordingly, trafficking of another COG-dependent toxin, SubAB[23], was also found to be sensitive to the localization of COG8; a significant fraction of SubAB-647 containing vesicles was redirected to mitochondria in cells that co-express COG8-mChActA and GFP-STX16 (Supplementary Figure S15).

STX16 trafficking is severely affected in COG8 deficient cells

STX16 is known to cycle between the *trans*-Golgi (TGN), endosomal membranes and the plasma membrane[24–26]. If COG8 plays a role in localization of STX16 vesicles, we would expect that STX16 trafficking would be disrupted in COG8 deficient cells. In wild-type HeLa cells, GFP-STX16 partially colocalizes with COG8 and GM130-positive Golgi membranes, and is also present on multiple puncta which are likely to represent endosomal compartments (Figure 7c and Supplementary Figure S4f). Strikingly, in COG8 depleted cells the majority of GFP-STX16 was found to relocalize to the plasma membrane (Figure 7d, e), supporting the hypothesis that COG8, and possibly the whole COG Lobe B sub-complex serves as a specific spatial landmark for STX16-carrying trafficking intermediates at the Golgi. Similarly, in COG8 deficient human fibroblasts endogenous STX16 was mislocalized from Golgi membranes (Supplementary Figure S16)

Discussion

The CATCHR sub-family of multi-subunit protein complexes has long been implicated in tethering of membrane trafficking intermediates at different steps of the secretory pathway[3] but the exact mechanism by which these complexes orchestrate vesicular approach, recognition, tethering, and fusion is still unclear. SNAREs are the major partner protein family for all CATCHR complexes[15, 16, 27–29], and subsequently it was proposed that one of the evolutionarily conserved functions of vesicle tethering complexes is to assist and/or stabilize SNARE complex formation. Indeed, the steady-state levels of assembled SNARE complexes was found to be significantly lower in cells deficient of COG complex subunits[15, 16].

In this work we have discovered several additional SNARE partners for the Golgi localized COG complex. In addition to the Qa SNARE STX5, previously shown to interact with COG4 and COG6[15], we have now discovered that the STX5 partner SNARE GS27 binds to both COG6 and COG8. These data suggest a role for the whole functional COG complex in the regulation of the *cis*-Golgi localized STX5 SNARE complex. Our data also demonstrated that the *trans*-Golgi Qa SNARE STX16 and its partner STX6 undergo specific protein-protein interactions with COG8 and COG6, implicating Lobe B of the COG complex in regulation of the STX16–centered *trans*-Golgi SNARE complex. These results were not limited to the HeLa cell model, as the COG4 recruitment of STX5 vesicles and the COG8 recruitment of STX16 vesicles to mitochondria was also observed in Vero cells

(Figure 6c–f). Additionally, Lobe B subunits can be specifically cross-linked to the endogenous STX16 (Supplementary Figure S17) further supporting the Lobe B-STX16 interaction data.

Yet another Golgi SNARE, SNAP29, was shown to interact with COG6, and to a lesser extent with COG8 and COG4 (Figure 1, Supplementary Figures S1 and S2). SNAP29 binds to STX6[30], forming a complex that is distinct from the well-studied STX16/STX6/Vti1/VAMP4 SNARE assembly, suggesting that COG may regulate an additional SNAP29/STX6-containing SNARE complex. In support of this hypothesis it was recently found that both SNAP29 and COG physically interact with the BLOC1 complex that is responsible for specialized cargo sorting in the endosome-to-Golgi retrograde trafficking pathway[31].

The exact nature of the COG-SNARE interactions (and CATCHR-SNARE interactions in general) is still under intense investigation. These interactions likely represent a multistep regulatory cascade in which different COG subunits simultaneously, and/or sequentially, interact with individual SNARE proteins and SNARE complexes before and during SNARE complex assembly. In vitro reconstitution experiments clearly demonstrate that target-to-target (t-t) SNARE sub-complexes are formed before the fusogenic *trans* vesicle-to-target (v-t) SNARE complexes[32, 33]. In this respect, the ability of different COG subunits to interact with different t-SNARE proteins may directly facilitate formation of t-t SNARE subcomplexes. For instance, simultaneous COG4-STX5 and COG6-GS27 interactions may facilitate the assembly of the STX5-GS27 intra-Golgi t-t SNARE subcomplex, while the concurrent COG8-STX16 and COG6-STX6 interactions would promote formation of the STX16-STX6 *trans*-Golgi t-t SNARE complex.

Additionally, the ability of different COG subunits to interact with the same SNARE protein may assist in the assembly of multiple SNARE complexes. It has been suggested that fusion of transport vesicles with target membranes is achieved by the simultaneous assembly of several SNARE complexes[34, 35]. Therefore, the ability of several COG subunits to interact with the same Qa SNARE (for instance, COG4, COG6 and COG8 with STX5) may facilitate the synchronized formation of a fusogenic array of SNARE complexes.

The most astonishing aspect of our studies is the finding that COG4 and COG8 proteins could specifically relocalize two different classes of SNARE-carrying trafficking intermediates in vivo. If transplanted to the outer mitochondria membrane, COG4 specifically attracts STX5-containing carriers, while COG8 prefers vesicles with STX16. To our knowledge this is the first example of the *in vivo* redirection of intra-Golgi trafficking carriers to other non-secretory cellular organelles.

This unusual COG-dependent relocalization of Qa SNAREs to mitochondria could be achieved by several possible scenarios. In the first scenario (a direct protein relocalization model), the co-expressed COG and SNARE partners could form a stable pair, prior to membrane insertion, which would be subsequently delivered to mitochondria. Indeed, direct COG-SNARE interactions were found to be essential for the efficient co-localization of proteins. However, these protein-protein interactions were not sufficient for relocalization of STX16 vesicles to mitochondria populated with COG8 truncation mutants that were

competent in STX16 binding (Figure 4g). Rapid redistribution of SNARE-containing vesicles to mitochondria observed in cell fusion experiments similarly indicate that redirected vesicular trafficking is the major cause of SNARE relocalization.

In the second scenario (an ER-mitochondria handshake model) newly synthesized ER SNARE proteins could be engaged in direct protein-protein interactions with the mitochondria anchored COG subunit, bringing the ER in a very close proximity to the mitochondrial membranes. Indeed, ER-mitochondria connections are well described[36–38], but we do not think that this scenario is playing a leading role in the COG-induced relocalization of membranes enriched in Golgi Qa SNAREs. ER located PDI does not generally colocalize with mitochondria-diverted GFP-STX5 or GFP-STX16 (Supplementary Figure S18). Additionally, we did not detect any colocalization between CFP-STX5 and GFP-Mff, the molecule that is specifically localized in ER-mitochondria contact sites[38] (Supplementary Figure S18). Finally, in cells that overexpress CFP-GalT, only the Golgi pool of CFP-GalT was found in a vicinity of COG4-bearing mitochondrial aggregates (Supplementary Figure S19), while the ER-localized pool of GalT-CFP[39] was not disturbed.

Most importantly though, the relocalization of SNARE-containing vesicles to mitochondria was regulated by the same components that were previously implicated in "normal" intra-Golgi trafficking. STX16 redirection to COG8-mitochondria was inhibited by overexpression of Vps45 (Figure 4g), while recruitment of STX5 vesicles to COG4-mitochondria required the presence of other COG subunits and participation of Sly1p (Supplementary Figure S9). In addition, STX5 recruitment to COG4-mitochondria was partially inhibited by BFA treatment (Supplementary Figure S20). These factors all indicate the active involvement of COPI-mediated vesicular trafficking in the relocalization process. Strikingly, in cells that express a modest level of COG4-mChActA, GFP-STX5 was mostly localized in vesicle-like punctate structures along the mitochondrial membranes (data not shown). Similar vesicular profiles were found in close proximity to mitochondrial membranes in TEM and Immuno-EM images (Figure 6), suggesting a third relocalization scenario (a vesicle re-routing model), in which mitochondria localized COG subunits serve as vesicle tethering platforms that are sufficient for capturing specialized classes of membrane trafficking intermediates. The COG4 platform includes other protein subunits from both Lobe A and Lobe B subcomplexes, while the COG8 platform is mostly enriched in Lobe B subunits. The two different COG platforms showed striking specificity for capturing either STX5 (COG4 platform), or STX16 (COG8 platform) containing vesicular carriers. STX5 vesicles were enriched in the ER-Golgi recycling marker ERGIC53 (Supplementary Figure S21), and are likely to represent *cis*/medial Golgi recycling carriers. On the other hand, STX16 vesicles partially colocalized with endocytosed Shiga toxin, and most likely represent endosome-to-Golgi recycling carriers (Figure 7a, b). We favor this latter vesicle relocalization scenario, however, the exact mechanism by which Qa SNARE-carrying transport intermediates are diverted to mitochondria will require additional investigation.

How can the data from the mitochondria relocalization assay be interpreted with regard to COG complex function in Golgi trafficking? We propose that, in addition to the direct facilitation of SNARE complex assembly, the essential function of the COG complex is to

serve as a spatial landmark for the localization of Qa SNAREs within Golgi subdomains. In this model, the complete COG complex determines the location of the *cis*/medial Qa SNARE STX5, while the Lobe B COG subcomplex, which exists as a separate entity in both soluble and membrane-bound forms, determines the position of the *trans* Qa SNARE STX16 (Figure 8). In support of this hypothesis we found that STX16 is severely mislocalized in cells deficient for COG8 (Figure 7e). This SNARE positioning function is likely to be conserved for all multisubunit tethering complexes.

In light of this model, there are numerous questions to be resolved, such as how the COG complex localizes itself onto Golgi subdomains, and are there major receptors for COG subcomplexes on the Golgi? These are crucial questions for future investigations. The development of the mitochondrial relocalization assay provides an excellent tool to address the biochemical requirements of the COG-mediated vesicle tethering process *in vivo*.

Methods

Reagents and antibodies

Protein G agarose were from Roche. Antibodies used for immunofluorescence (IF) microscopy or western blotting (WB) were purchased through commercial sources, gifts from generous individual investigators, or generated by us via affinity purification. Antibodies were as follows:

Rabbit polyclonal: Myc (Bethyl Laboratories); COG3, COG4, COG6, COG8 (this lab); GS27 (Synaptic Systems); Giantin (Covance); TGN46 (AbD Serotech).

Mouse monoclonal: GFP (Molecular Probes); GFP (Covance); GM130 (BD Biosciences); p115; GPP130 (Alexis); PDI (Affinity Bio Reagents); ERGIC53 (Enzo Life Sciences); Ox Phos ComplexV (Invitrogen); Myc (Cell Signaling).

Secondary IRDye 680 goat anti-rabbit, IRDye 700 goat anti-mouse and IRDye 800 donkey anti-goat for WB were from LI-COR Biosciences. Anti-rabbit HiLyte 488, HiLyte 555, and DyLight647 for IF were obtained from AnaSpec and Jackson ImmunoResearch, Inc.

Cell culture

HeLa cells were cultured in DMEM/F-12 medium (Thermo Scientific) supplemented with 15 mM HEPES, 2.5 mM L-glutamine and 10% FBS (Atlas Biologicals) at 37°C and 5% CO_2 in a 90% humidified incubator. GFP-COG6 stable cell lines were generated by transfecting cells with pEGFP-C1-COG6 followed by selection for G418 resistance in complete medium supplemented with 0.4 mg/mL G418 sulfate. YFP-COG3 stable cell lines were generated as described[15].

siRNA-induced knockdowns

siRNA duplexes for COG1 (D-013309-01(UAGAUGACCUCCUGGCUUA) and D-013309-04 (GUAGCGGCCUCUCCAUGAA)), COG2, COG3, COG4, and COG8[12, 21, 23] were obtained from Dharmacon (Chicago, IL). Transfection was performed

using lipofectamine RNAiMAX siRNA Transfection Reagent (Invitrogen) and cells were analyzed 72 h after transfection.

Plasmid preparation and transfection

Yeast and mammalian expression constructs were generated using standard molecular biology techniques or obtained as generous gifts (Table 1).

Yeast two hybrid: cDNA constructs expressing SNAREs were from Open Biosystems. DNA fragments encoding cytoplasmic domains of SNAREs were subcloned into pGBDU vector as EcoR1/Sal1 or BglII/Xho1 inserts and verified by sequencing.

IF/IP: Human COG8 with deletions of amino acids 8–148 and 8–436 were generated by PCR using hCOG8-pEGFP as a template. hCOG1 (898–980) was generated by PCR and subcloned into pCDNA3.1 (BamHI/Xho1). To generate fluorescently-tagged chimeras full-length proteins were inserted into pECFP-C1, pEGFP-C1 (BspE1/BamHI) or pmCherry-C1-ActA (BspE1/NdeI) vectors. pEGFP-C1-STX16 deletions aa 2–73 or 2–169 were generated by PCR using pEGFP-C1-STX16 as a template. To generate STX5-mChActA and STX16-mChActA cytoplasmic domains of rSTX5a and hSTX16 were amplified by PCR and subcloned into pmCherry-C1-ActA vector.

Plasmids were isolated from bacterial cells using the QIAprep Spin Miniprep Kit (Qiagen). Plasmid transfections into tissue culture cells were performed with Lipofectamine 2000 (Invitrogen).

Immunofluorescence microscopy

Cells were grown on glass coverslips one day before transfection. After transfection cells were fixed and stained as described previously[12]. Cells were imaged with the 63X oil 1.4 NA objective of a LSM510 Zeiss Laser inverted microscope outfitted with confocal optics. Image acquisition was controlled with LSM510 software (Release Version 4.0 SP1). The "RGB profiler" plug-in of Image J (http://rsbweb.nih.gov/ij) was used to generate line plots for individual channels. The "Coloc_2" plug-in was utilized to calculate Pearson coefficient for co-localization. At least three independent experiments were performed to calculate both mean and standard deviation values.

SDS–PAGE and Western blotting

SDS–PAGE and WB were performed as previously described [14]. Blots were incubated with primary antibodies, and then with a secondary antibody conjugated with IRDye 680 or IRDye 800 dyes. Blots were scanned and analyzed with an Odyssey Infrared Imaging System (LI-COR). At least three independent experiments were performed to calculate both mean and standard deviation values.

Yeast two-hybrid assay

The following constructs were used in yeast two-hybrid assay: COG subunits (1–8) of mammalian COG complex were cloned as C-terminal fusion constructs with Gal4 AD and SNARE constructs lacking transmembrane domain were cloned as C-terminal fusion

constructs with Gal4 BD by recombination cloning in yeast. The Gal4 two-hybrid system was used as described[18, 40]. Reporter strains of opposite mating types were transformed with bait and prey fusion constructs. Growth of independent transformants was assessed on media lacking leucine (prey fusions) and uracil (bait fusions). Diploid yeasts containing combinations of the human COG subunits 1–8 and SNAREs, as well as empty vectors and pair-wise combinations of human COG2/4 [11]) were created by mass mating. Yeast diploids were selected on –LEU/–URA plates. Diploids were grown in liquid –Leu/–Ura medium to the same optical density (D600 = 0.8) and titrated 1:10, 1:100, 1:1,000, and 1:10,000 in ddH$_2$O. 5 µl of each dilution was applied on a selective medium lacking adenine, histidine, and leucine/uracil, incubated at 30°C for 72 h, and scored for growth. Expression of all hybrid molecules was verified by WB. The relative stringency of direct protein–protein interaction was estimated by growth assay on agar plates lacking either histidine (–HIS; leaky regulation) or adenine (–ADE; high stringency regulation).

Immunoprecipitations

Cells were collected and lysed in a 1% Triton X-100 PBS buffer with 10µL/mL of 100X Halt protease inhibitor cocktail for 1hr on ice. Post-nuclear supernatant was cleared and 90% was added to GFP antibodies and incubated on ice overnight. Next day, protein G agarose beads (Roche) was added to each reaction and samples incubated at 4°C on a rotator for 2h. Unbound material was removed, beads were washed 4X in 0.05% Triton X-100 in PBS and eluted in 2X sample buffer.

Fluorescence Recovery after photobleaching

HeLa cells grown on glass-bottom culture plates were transiently transfected with COG8-mChActA and GFP-STX16 plasmids. FRAP was performed using a laser-scanning confocal microscope (LSM 710 Zeiss Laser inverted microscope outfitted with confocal optics) equipped with an environmental control system (Live cell system, Biovision technologies) set to 37°C and 5% CO$_2$. Cells were cultured in phenol red–free DMEM/F12 (Sigma-Aldrich) with 1% FBS. Prebleached images were taken for 12sec (7sec/frame), and the selected mitochondria area was bleached for 5sec using a pulse of the 488-nm and 561-nm laser lines at maximal intensity and 15 iterations/ROI. After bleaching, fluorescence images were then recorded every 7sec for 6min 45sec.

Transmission Electron Microscopy

Samples were treated according to Valdivia's lab protocol[41] with modifications. In short, cells were fixed for 20 min on ice with 2.5% glutaraldehyde and 0.05% malachite green (EMS) in 0.1M sodium cacodylate buffer, pH 6.8. Samples were post-fixed for 30 min at room temperature with 0.5% osmium tetroxide and 0.8% potassium ferricyanide in 0.1 M sodium cacodylate, for 20 min on ice in 1% tannic acid, and for 1 h in 1% uranyl acetate at room temperature. Specimens were dehydrated with a graded ethanol series, and embedded in Araldite 502/Embed 812 resin (EMS). Ultrathin sections were imaged at 80 kV on a FEI Technai G2 TF20 transmission electron microscope and images were acquired with a FEI Eagle 4kX USB Digital Camera.

Immuno-Electron Microscopy

Vero cells were co-transfected with COG4-mChActA and GFP-STX5. 20h after transfection cells were washed in PBS and fixed in 4% paraformaldehyde for 30 min. After washing in 50 mM NH_4Cl in PBS for 5 min cells were blocked in 1% BSA, 0.1% saponin in PBS solution twice for 10 min at RT. Cells were exposed to rabbit anti-GFP antibodies (1:500) in 1% fish gelatin, 0.1% saponin in PBS for 2 hrs at RT, washed in 0.005% saponin in PBS, and then incubated with the Fab' fragment of a goat anti-rabbit IgG conjugated to colloidal gold (1.4 nm in diameter, Nanoprobes) in 0.005% saponin in PBS for 2 hrs. The cells were fixed in 1% glutaraldehyde in PBS for 10 min washed in 50 mM glycin in PBS, 1% BSA in PBS, and H_2O. The gold labeling was intensified with a gold enhancement kit GoldEnhance-EM (Nanoprobes) for 2 min following the manufacturer's protocol. After rinsing cells in 1% aqueous sodium thiosulfate and H_2O, the cells were postfixed in PBS containing 1% OsO_4 and 1.5% potassium ferrocyanide for 60 min, washed in H_2O, dehydrated in a series of graded ethanol solutions, and embedded in Araldite 502/Embed 812 resin (EMS).

Toxin trafficking assay

Cells were grown on glass coverslips one day before transfection. After transfection cells were washed with cold PBS and incubated on ice with Alexa Fluor 647 labeled Shiga toxin B subunit (STB647) or Subtilase cytotoxin (SubAB647) for 20 min. Cells were washed to remove unbound toxin and incubated with fresh media at 37°C for 1h. Cells were then fixed and prepared for IF staining as indicated above. Toxins were labeled according to manufacturer's protocol (Invitrogen).

Cell fusion assay

Transiently transfected Vero cells were grown on coverslips andimaged using a laser confocal spinning disk microscope system based on a Nikon TiE microscope, equipped with a Yokogawa CSU-X1 and an Andor iXon+ EMCCD camera and fitted with 40×, 1.30 NA and 100×, 1.49 NA objectives. Image acquisition was controlled with Andor Bioimaging software (Andor IQ2.1). After start of time lapse image acquisition, cell-cell fusion was mediated by a HVJ envelope cell fusion kit (GenomeONE-CF EX; Cosmo Bio Co.). For cell fusion to occur, cells were washed once with 'cell fusion buffer' following the manufacturer's protocol and incubated for 10 min with a 1:40 dilution of the HVJ envelope solution, leading to efficient fusion of cells contacting each other.

Supplementary Material

Refer to Web version on PubMed Central for supplementary material.

Acknowledgements

Abbreviations

COG   conserved oligomeric Golgi

mCh   mCherry

SNARE   soluble N-ethylmalemide-sensitive fusion attachment protein receptor

References

1. Bonifacino JS, Glick BS. The mechanisms of vesicle budding and fusion. Cell. 2004; 116:153–166. [PubMed: 14744428]

2. Cottam NP, Ungar D. Retrograde vesicle transport in the Golgi. Protoplasma. 2011

3. Yu IM, Hughson FM. Tethering factors as organizers of intracellular vesicular traffic. Annu Rev Cell Dev Biol. 2010; 26:137–156. [PubMed: 19575650]

4. Brown FC, Pfeffer SR. An update on transport vesicle tethering. Mol Membr Biol. 2010; 27:457–461. [PubMed: 21067454]

5. Lupashin V, Sztul E. Golgi tethering factors. Biochimica Et Biophysica Acta-Molecular Cell Research. 2005; 1744:325–339.

6. Epp N, Rethmeier R, Kramer L, Ungermann C. Membrane dynamics and fusion at late endosomes and vacuoles--Rab regulation, multisubunit tethering complexes and SNAREs. Eur J Cell Biol. 2011; 90:779–785. [PubMed: 21683469]

7. Miller VJ, et al. Molecular insights into vesicle tethering at the Golgi by the Conserved Oligomeric Golgi (COG) complex and the golgin TMF. J Biol Chem. 2012 **Epub ahead of print**.

8. Whyte JR, Munro S. The Sec34/35 Golgi Transport Complex Is Related to the Exocyst, Defining a Family of Complexes Involved in Multiple Steps of Membrane Traffic. Developmental Cell. 2001; 1:527–537. [PubMed: 11703943]

9. Ungar D, et al. Characterization of a mammalian Golgi-localized protein complex COG that is required for normal Golgi morphology and function. Journal of Cell Biology. 2002; 157:405–415. [PubMed: 11980916]

10. Fotso P, Koryakina Y, Pavliv O, Tsiomenko AB, Lupashin VV. Cog1p plays a central role in the organization of the yeast conserved oligomeric golgi complex. Journal of Biological Chemistry. 2005; 280:27613–27623. [PubMed: 15932880]

11. Ungar D, Oka T, Vasile E, Krieger M, Hughson FM. Subunit architecture of the conserved oligomeric golgi complex. Journal of Biological Chemistry. 2005; 280:32729–32735. [PubMed: 16020545]

12. Pokrovskaya ID, et al. Conserved oligomeric Golgi complex specifically regulates the maintenance of Golgi glycosylation machinery. Glycobiology. 2011; 21:1554–1569. [PubMed: 21421995]

13. Foulquier F. COG defects, birth and rise! Biochim Biophys Acta. 2009; 1792:896–902. [PubMed: 19028570]

14. Suvorova ES, Duden R, Lupashin VV. The Sec34/Sec35p complex, a Ypt1p effector required for retrograde intra-Golgi trafficking, interacts with Golgi SNAREs and COPI vesicle coat proteins. Journal of Cell Biology. 2002; 157:631–643. [PubMed: 12011112]

15. Shestakova A, Suvorova E, Pavliv O, Khaidakova G, Lupashin V. Interaction of the conserved oligomeric Golgi complex with t-SNARE Syntaxin5a/Sed5 enhances intra-Golgi SNARE complex stability. J Cell Biol. 2007; 179:1179–1192. [PubMed: 18086915]

16. Laufman O, Hong W, Lev S. The COG complex interacts directly with Syntaxin 6 and positively regulates endosome-to-TGN retrograde transport. J Cell Biol. 2011; 194:459–472. [PubMed: 21807881]

17. Sengupta D, Truschel S, Bachert C, Linstedt AD. Organelle tethering by a homotypic PDZ interaction underlies formation of the Golgi membrane network. J Cell Biol. 2009; 186:41–55. [PubMed: 19581411]

18. Kudlyk T, Willett R, Pokrovskaya ID, Lupashin V. COG6 interacts with a subset of the Golgi SNAREs and is important for the Golgi complex integrity. Traffic. 2012 **Epub ahead of print**.

19. Laufman O, Kedan A, Hong W, Lev S. Direct interaction between the COG complex and the SM protein, Sly1, is required for Golgi SNARE pairing. Embo J. 2009; 28:2006–2017. [PubMed: 19536132]

20. Orci L, Perrelet A, Rothman JE. Vesicles on strings: morphological evidence for processive transport within the Golgi stack. Proc Natl Acad Sci U S A. 1998; 95:2279–2283. [PubMed: 9482876]

21. Zolov SN, Lupashin VV. Cog3p depletion blocks vesicle-mediated Golgi retrograde trafficking in HeLa cells. Journal of Cell Biology. 2005; 168:747–759. [PubMed: 15728195]

22. Amessou M, et al. Syntaxin 16 and syntaxin 5 are required for efficient retrograde transport of several exogenous and endogenous cargo proteins. J Cell Sci. 2007; 120:1457–1468. [PubMed: 17389686]

23. Smith RD, et al. The COG complex, Rab6 and COPI define a novel Golgi retrograde trafficking pathway that is exploited by SubAB toxin. Traffic. 2009; 10:1502–1517. [PubMed: 19678899]

24. Simonsen A, Bremnes B, Ronning E, Aasland R, Stenmark H. Syntaxin-16, a putative Golgi t-SNARE. Eur J Cell Biol. 1998; 75:223–231. [PubMed: 9587053]

25. Chen Y, Gan BQ, Tang BL. Syntaxin 16: unraveling cellular physiology through a ubiquitous SNARE molecule. J Cell Physiol. 2010; 225:326–332. [PubMed: 20589833]

26. Shewan AM, et al. GLUT4 Recycles via a trans-Golgi Network (TGN) Subdomain Enriched in Syntaxins 6 and 16 But Not TGN38: Involvement of an Acidic Targeting Motif. Mol Biol Cell. 2003; 14:973–986. [PubMed: 12631717]

27. Perez-Victoria FJ, Bonifacino JS. Dual roles of the mammalian GARP complex in tethering and SNARE complex assembly at the trans-golgi network. Mol Cell Biol. 2009; 29:5251–5263. [PubMed: 19620288]

28. Sivaram MV, Saporita JA, Furgason ML, Boettcher AJ, Munson M. Dimerization of the exocyst protein Sec6p and its interaction with the t-SNARE Sec9p. Biochemistry. 2005; 44:6302–6311. [PubMed: 15835919]

29. Kraynack BA, et al. Dsl1p, Tip20p, and the novel Dsl3(Sec39) protein are required for the stability of the Q/t-SNARE complex at the endoplasmic reticulum in yeast. Mol Biol Cell. 2005; 16:3963–3977. [PubMed: 15958492]

30. Wong SH, et al. GS32, a novel Golgi SNARE of 32, kDa interacts preferentially with syntaxin 6. Mol Biol Cell. 1999; 10:119–134. [PubMed: 9880331]

31. Gokhale A, et al. Quantitative Proteomic and Genetic Analyses of the Schizophrenia Susceptibility Factor Dysbindin Identify Novel Roles of the Biogenesis of Lysosome-Related Organelles Complex 1. J. Neurosci. 2012; 32:3697–3711. [PubMed: 22423091]

32. Söllner T, Bennett MK, Whiteheart SW, Scheller RH, Rothman JE. A protein assembly-disassembly pathway *in vitro* that may correspond to sequential steps of synaptic vesicle docking, activation, and fusion. Cell. 1993; 75:409–418. [PubMed: 8221884]

33. Parlati F, et al. Topological restriction of SNARE-dependent membrane fusion [see comments]. Nature. 2000; 407:194–198. [PubMed: 11001058]

34. Mohrmann R, de wit H, Verhage M, Neher E, Sorensen JB. Fast vesicle fusion in living cells requires at least three SNARE complexes. Science. 2010; 330:502–505. [PubMed: 20847232]

35. Hua Y, Scheller RH. Three SNARE complexes cooperate to mediate membrane fusion. Proc Natl Acad Sci U S A. 2001; 98:8065–8070. [PubMed: 11427709]

36. Giorgi C, De Stefani D, Bononi A, Rizzuto R, Pinton P. Structural and functional link between the mitochondrial network and the endoplasmic reticulum. Int J Biochem Cell Biol. 2009; 41:1817–1827. [PubMed: 19389485]

37. de Brito OM, Scorrano L. Mitofusin 2 tethers endoplasmic reticulum to mitochondria. Nature. 2008; 456:605–610. [PubMed: 19052620]

38. Friedman JR, et al. ER tubules mark sites of mitochondrial division. Science. 2011; 334:358–362. [PubMed: 21885730]

39. Rhee SW, Starr T, Forsten-Williams K, Storrie B. The steady-state distribution of glycosyltransferases between the Golgi apparatus and the endoplasmic reticulum is approximately 90:10. Traffic. 2005; 6:978–990. [PubMed: 16190979]

40. James P, Halladay J, Craig EA. Genomic libraries and a host strain designed for highly efficient two-hybrid selection in yeast. Genetics. 1996; 144:1425–1436. [PubMed: 8978031]

41. Cocchiaro JL, Kumar Y, Fischer ER, Hackstadt T, Valdivia RH. Cytoplasmic lipid droplets are translocated into the lumen of the Chlamydia trachomatis parasitophorous vacuole. Proc Natl Acad Sci U S A. 2008; 105:9379–9384. [PubMed: 18591669]
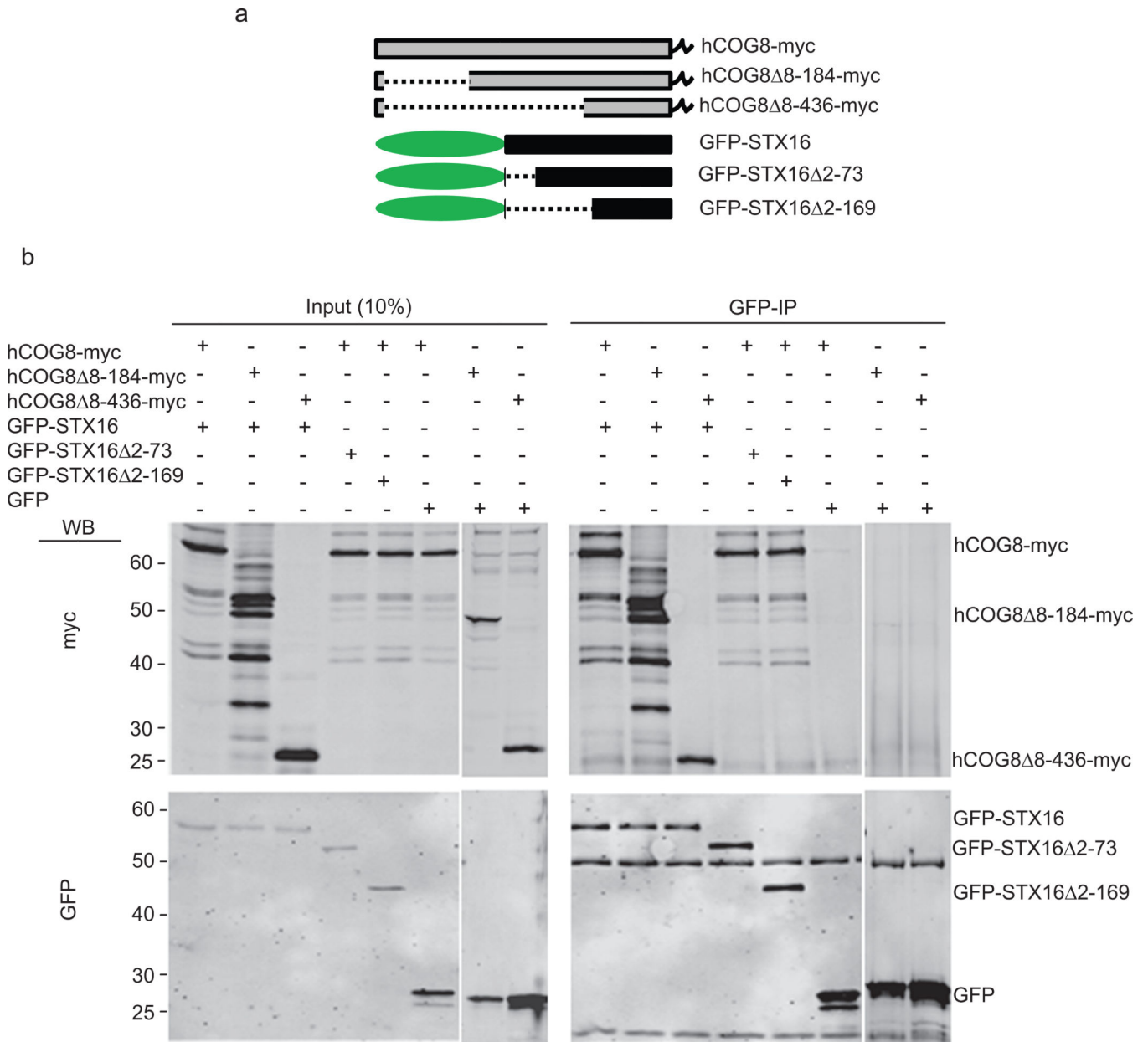
Author Manuscript

Author Manuscript

Author Manuscript

Author Manuscript

Figure 1. COG8 C terminus interacts with SNARE domain of STX16

HeLa cells transiently co-transfected with plasmids encoding fluorescent tagged SNAREs and COG-myc constructs as indicated (**a**). 24 h post-transfection, cells were collected, lysed, and GFP-SNARE interacting proteins were precipitated with anti-GFP antibodies. Immuno-precipitates, along with 10% of total input, were separated on a 12% SDS-PAGE gel, transferred to nitrocellulose membrane, and probed with antibodies against myc (**b**, upper panel) and GFP (**b**, lower panel). COG8 8–184-myc and COG8 8–436-myc are still capable of interaction with full length GFP-STX16. GFP-STX16 truncated mutants missing either the N terminus (GFP-STX16 2–73) or N terminus and Habc domain (GFP-STX16 2–169) are both still capable of interaction with full length COG8-myc.
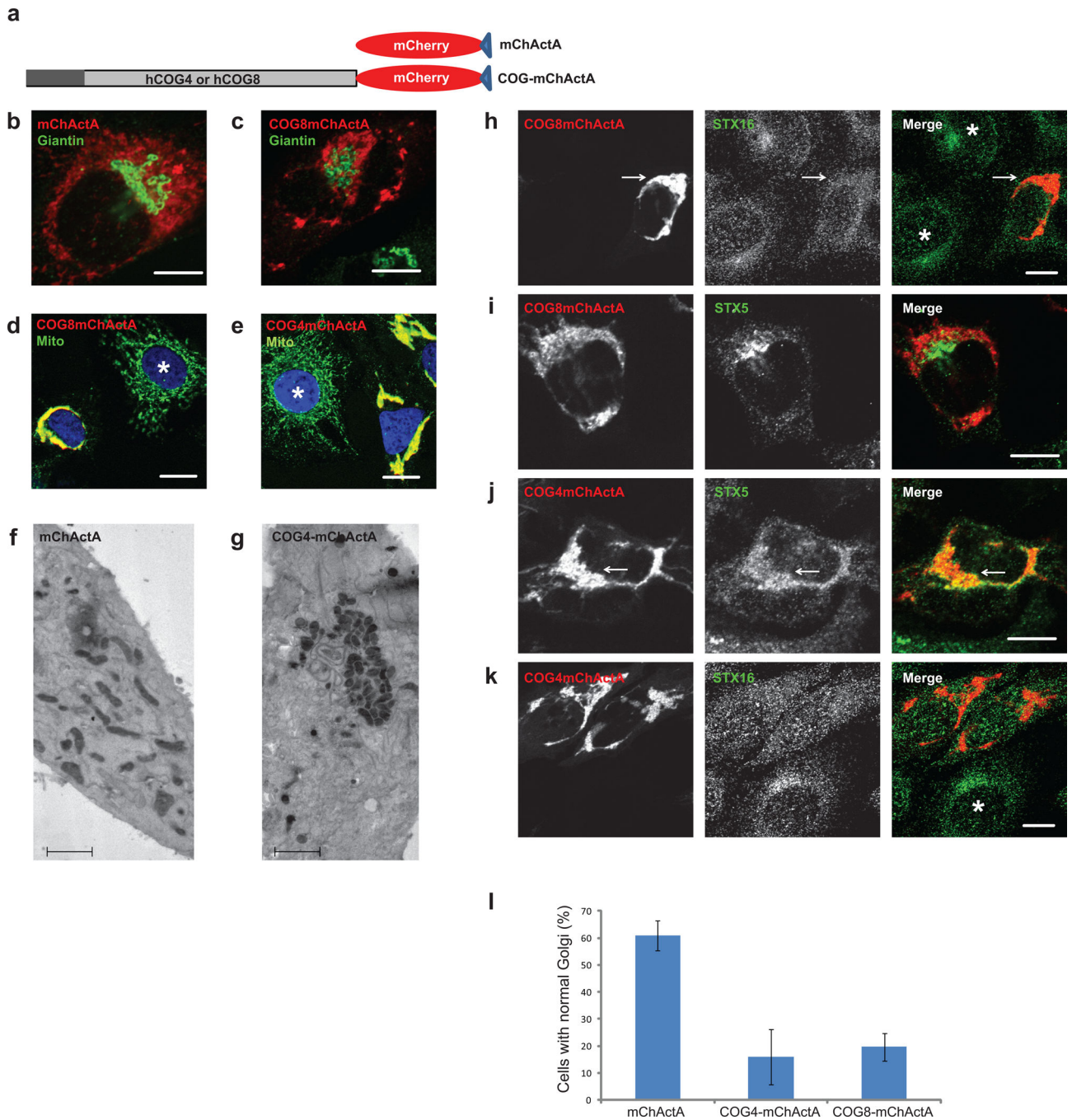
Figure 2. Mitochondrial clustering and Golgi fragmentation in cells expressing COG subunits on mitochondria

A schematic diagram of the mitochondrial targeting protein constructs (**a**). HeLa cells expressing mChActA (**b, f**), COG8-mChActA (**c, d**), or COG4-mChActA (**e, g**) were analyzed 24 h after transfection using confocal or TEM microscopy. Cells were stained with antibodies to Giantin (**b, c**) to identify Golgi, or mitochondria resident protein Ox Phos ComplexV (**d, e**) to image mitochondria. Mitochondria are not clustered in untransfected cells (**d, e**, asterisk), or in cells expressing mChActA (**b, f**), and clustered in cells expressing

COG8-mChActA (**c**, **d**) or COG4-mChActA (**e**, **g**). Using a gene replacement strategy, cells were depleted of COG8 (**h**, **i**) or COG4 (**j**, **k**) using siRNA transfection. 72 h after knockdown cells were transfected with siRNA resistant COG8-mChActA (**h**, **i**) or COG4-mChActA (**j**, **k**), 24 h later cells were stained with antibodies to STX16 (**h**, **k**) or STX5 (**i**, **j**) (asterisk denotes non transfected cell). Endogenous STX16 is partially mislocalized to COG8 labeled mitochondria (**h**), while endogenous STX5 shows co-localization with COG4-clustered mitochondria (**j**). Quantification of the Golgi disruption phenotype in cells expressing mitochondria-targeted COG subunits (**l**). HeLa cells plated on coverslips were transfected with plasmids encoding either mChActA, COG4-mChActA, or COG8-mChActA. 24 hrs after transfection, cells were fixed and stained with antibodies against GM130 and analyzed using confocal microscopy, Size bars; IF-10 μm, TEM 2 μm. Golgi fragmentation was scored by evaluation of Golgi morphology based on GM130 signal in transfected cells. Averages of three independent measurements, mChActA n=66, COG4-mChActA n=44, COG8-mChActA n=38. Error bars denote standard deviation from average.
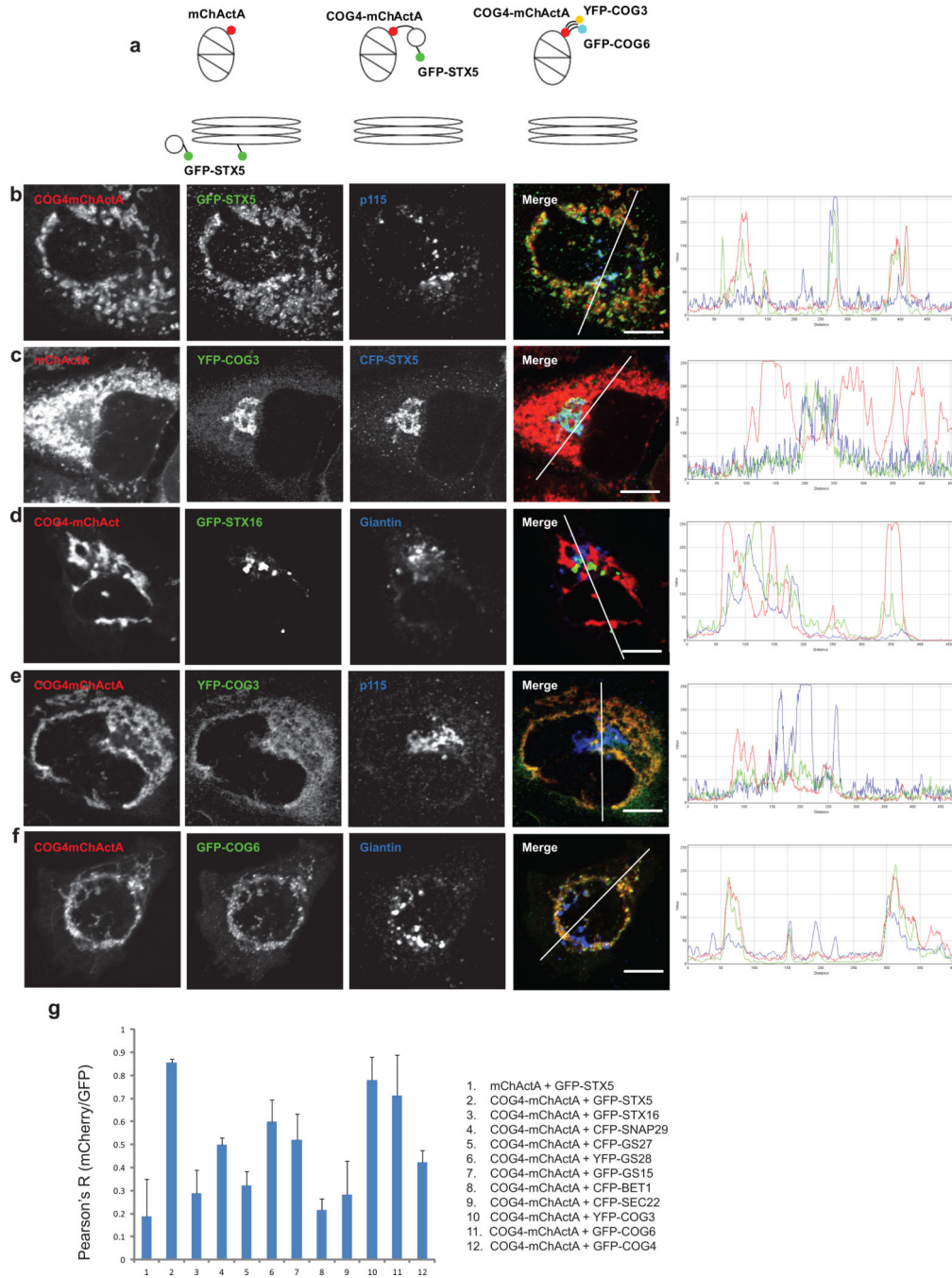
Figure 3. Mitochondria-targeted COG4 relocates STX5 membranes and attracts Lobe A and B COG subunits

A schematic diagram of the mitochondrial targeting protein constructs (**a**). HeLa cells transiently expressing GFP-STX5 (**b**), CFP-STX5 (**c**), GFP-STX16 (**d**), or stably expressing YFP-COG3 (**c, e**), or GFP-COG6 (**f**), were transfected with a plasmid encoding either mChActA (**c**) or COG4-mChActa (**b, d–f**). 24 h after transfection cells were fixed, and then stained with antibodies to Giantin or p115 as indicated, and analyzed by confocal microscopy. Line plots for overlap between red, green and blue channels are shown

measuring the relative value of signal intensity (y-axis) over the distance measured in pixels (x-axis). Size bar, 10 μm. Plot for the average Pearson coefficient for colocalization between mCherry/red and GFP/green signal for indicated constructs and proteins (**g**) error bars represent standard deviation, n 3.
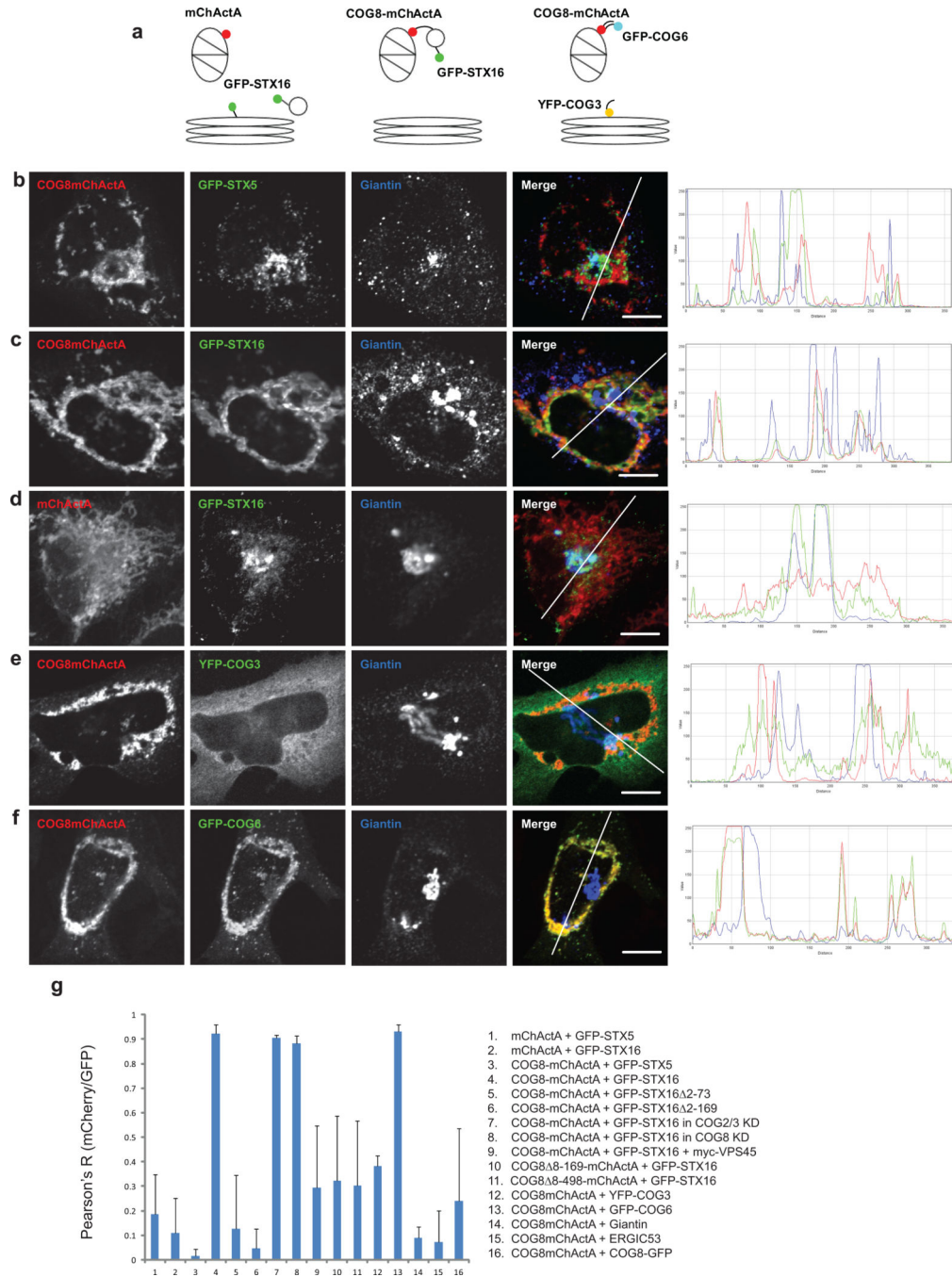
Figure 4. Mitochondria-targeted COG8 relocates STX16 vesicles and attracts obe B COG subunits

A schematic diagram of the mitochondrial targeting protein constructs (**a**). HeLa cells transiently expressing GFP-STX5 (**b**), GFP-STX16 (**c, d**), or stably expressing YFP-COG3 (**e**), or GFP-COG6 (**f**), were transfected with a plasmid encoding either mChActA (**d**) or COG8-mChActa (**b, c, e, f**). 24 h after transfection cells were fixed, stained with antibodies to Giantin, and analyzed by confocal microscopy. Line plots for overlap between red, green and blue channels are shown measuring the relative value of signal intensity (y-axis) over

the distance measured in pixels (x-axis). Size bar, 10 µm. Plot for the average Pearson coefficient for colocalization between mCherry/red and GFP/green signal for the indicated constructs and proteins (**g**) error bars represent standard deviation, n 3.
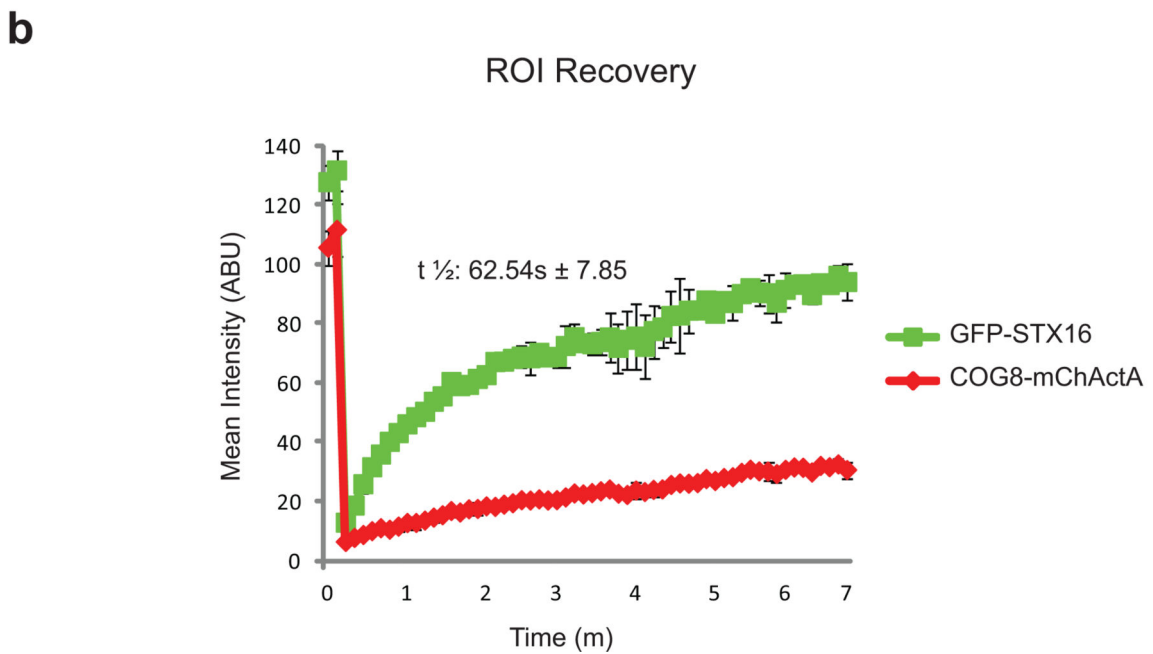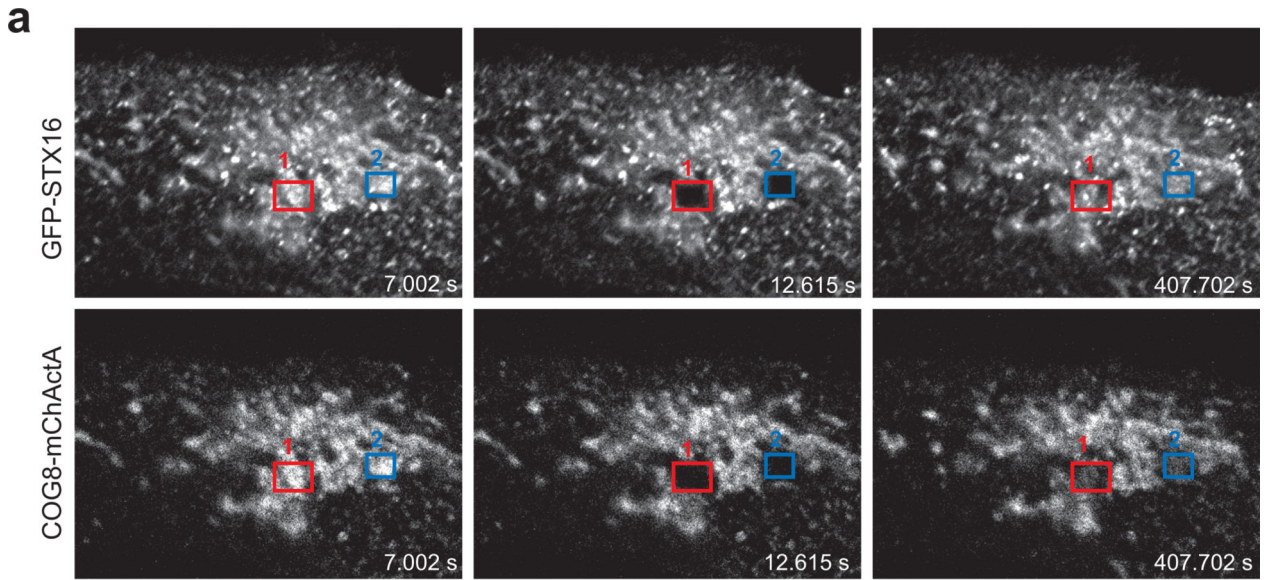
**Figure 5. GFP-STX16 containing membranes cycle rapidly on/off COG8-mChActA labeled mitochondria**

HeLa cells transiently expressing COG8-mChActA and GFP-STX16 were incubated at 37°C and visualized with a LSM710 laser confocal microscope. Both COG8-mChActA and GFP-STX16 were bleached and their FRAP was measured over a course of 7 minutes. Representative frames for pre-bleached and post-bleached time points are shown (**a**). FRAP of COG8-mChActA was slower compared to GFP-STX16 which had a $t_{1/2}$ of 62.54 seconds (**b**), average from two experiments.
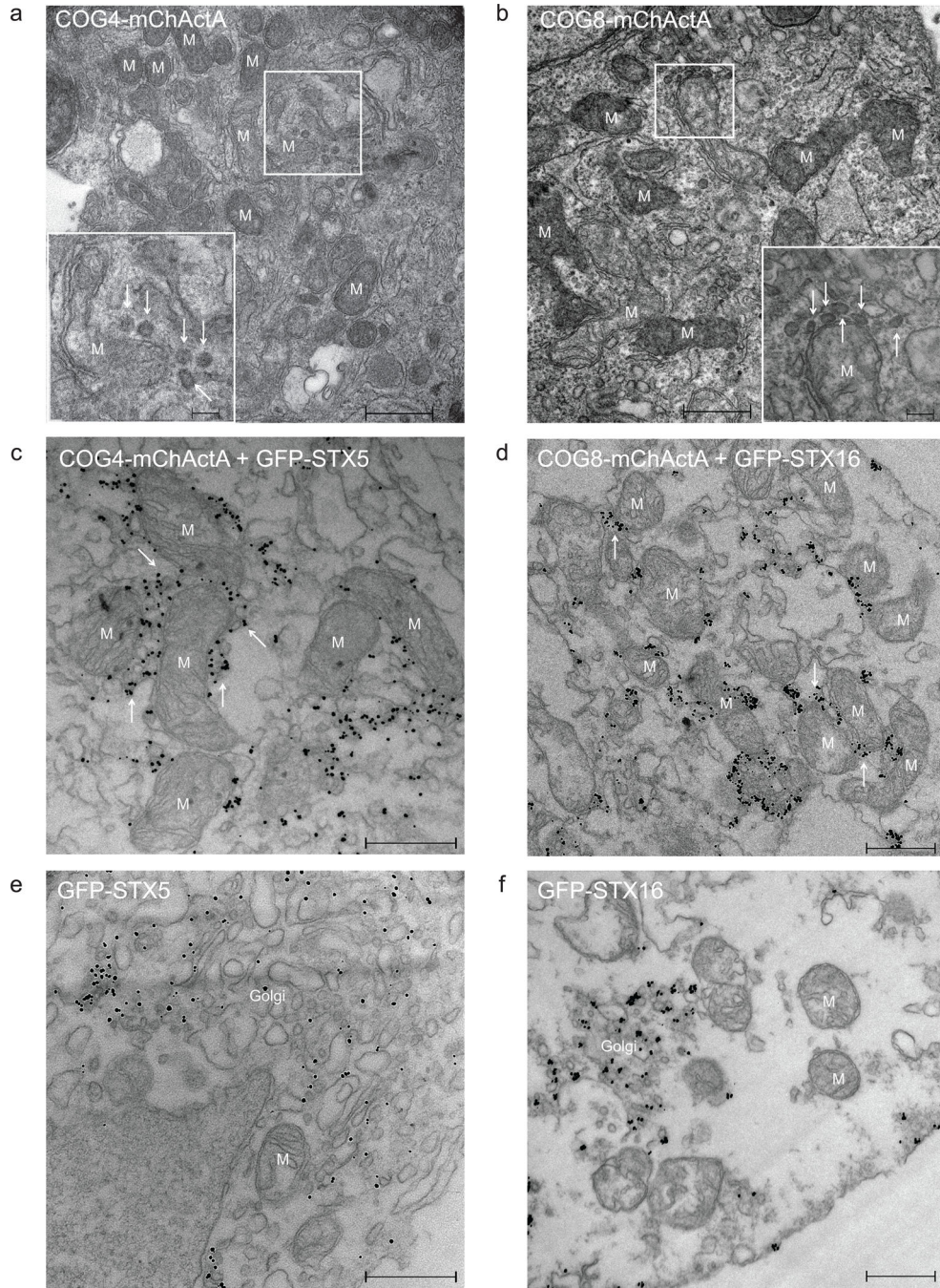
Figure 6. Vesicles associate with mitochondria in cells expressing COG8 or COG4 targeted to mitochondria

Electron micrograph of HeLa (**a, b**) and Vero (**c–f**) cells transiently transfected with COG4-mChActa (**a**), COG8-mChActA (**b**), COG4-mChActA + GFP-STX5 (**c**), COG8-mChActA + GFP-STX16 (**d**), mChActA + GFP-STX5 (**e**), mChActA + GFP-STX16 (**f**). 24 h after transfection cells were fixed and processed for TEM (**a, b**) or immuno-EM (**c–f**). The inset shows a high magnification view of vesicular profiles. Mitochondria (M) and mitochondria-associated vesicles (see arrows) are indicated. Size bar, 500 nm (inset 100nm).
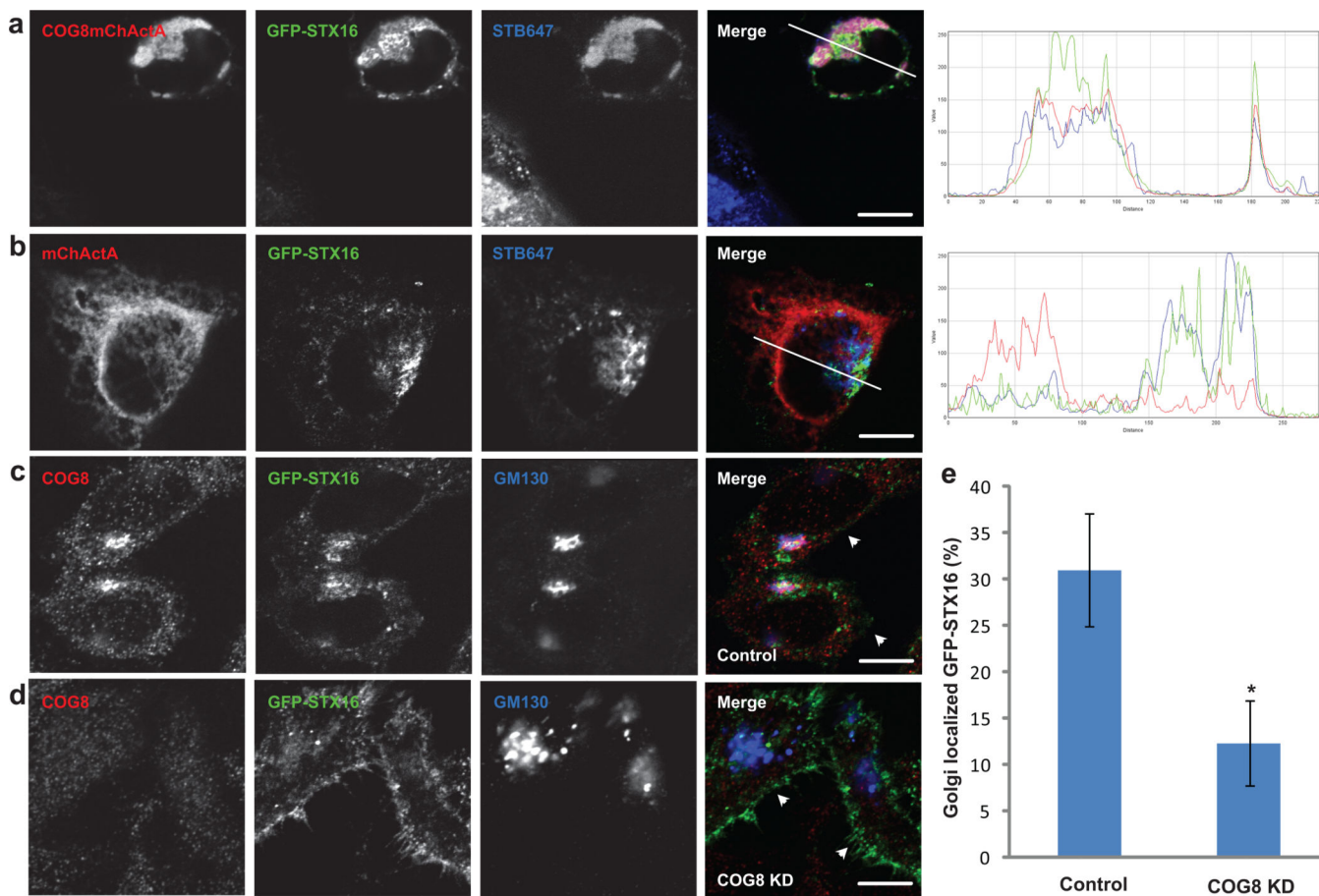
Figure 7. COG8 is required for localization of STX16 containing trafficking intermediates
HeLa cells were co-transfected with plasmids encoding COG8-mChActa and GFP-STX16
(**a**), or mChActA and GFP-STX16 (**b**). 20 h after transfection cells were pulsed with
Alexa647 labeled STB (STB647) for 20 min, then washed and additionally chased in fresh
media for 2 h. Cells were fixed, and analyzed by confocal microscopy. HeLa cells were
transfected with GFP-STX16 (**c**), or co-transfected with GFP-STX16 and COG8 siRNA (**d**)
by electroporation. After 72 h cells were fixed, stained with COG8 and GM130 antibodies,
and analyzed using confocal microscopy. White arrows indicate change in localization of
GFP-STX16 from GM130 labeled Golgi membranes to the plasma membrane. Quantitative
analysis (**e**) performed as follows; Control n=24, COG8 KD n=31, error bars represent
standard deviation. STX16 fluorescence was measured using ImageJ software and
measuring GFP-STX16 signal in GM130 labeled Golgi ROI and around the total cell.
Students t-test was used to calculate p value. * p=4.86E-18. Size bar, 10 μm.
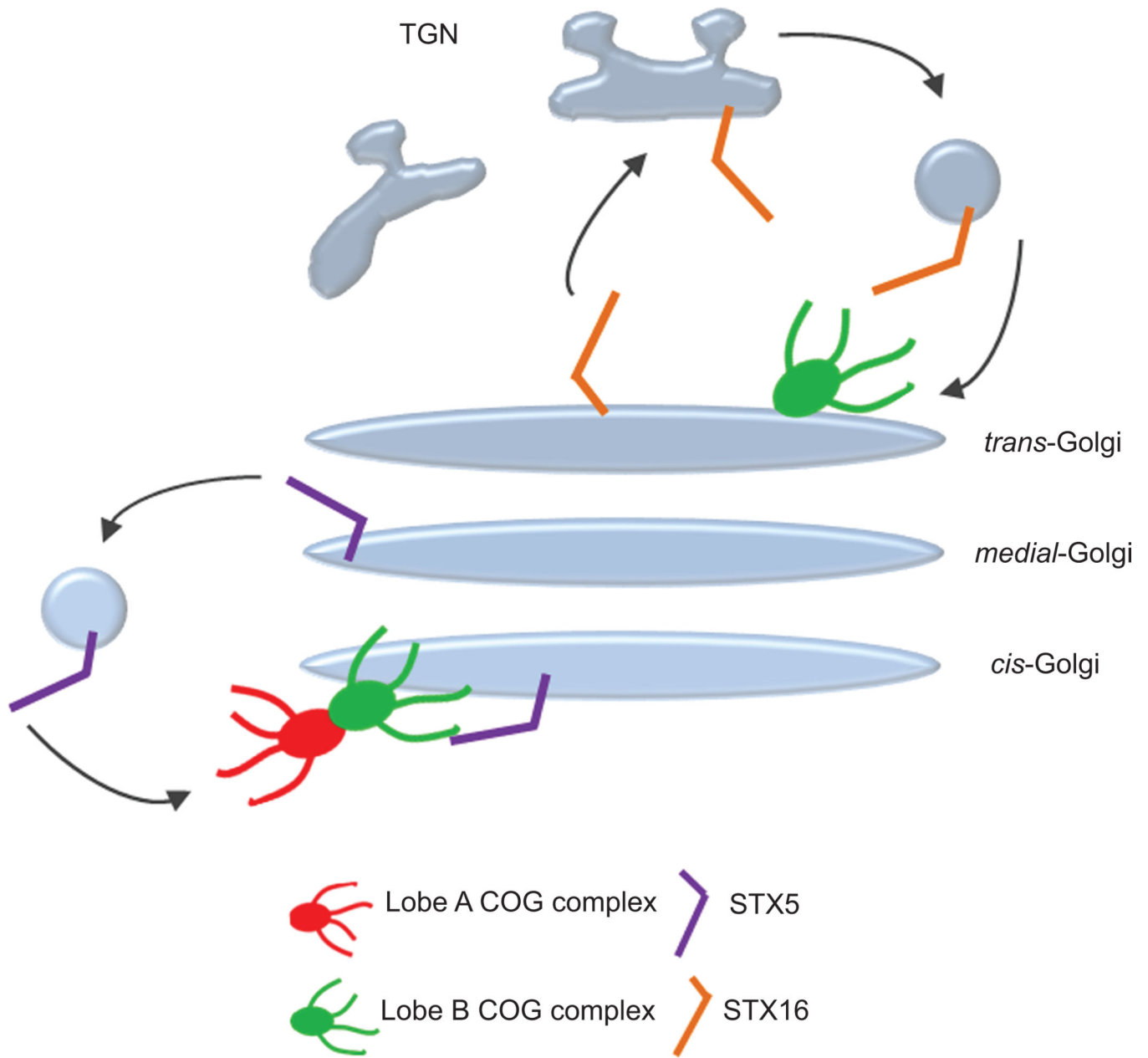
Figure 8. COG complex serves as a spatial landmark for precise localization of Qa SNAREs in Golgi subdomains

Hypothetical model of how the COG complex functions in organizing different SNARE complexes on Golgi membranes. The recycling STX5 containing SNARE complex (purple rod) is targeted by both lobe A and lobe B of the COG complex to direct it to *cis* Golgi membranes. The TGN localized STX16 containing SNARE complex (orange rod) is targeted by lobe B of the COG complex to direct it to *trans* Golgi membranes.

Table 1

SNAREs interact with COG4, COG6 and COG8 subunits

Yeast two-hybrid assay. Yeast diploids co-expressing Gal4 AD-hCOG1-8 fusions and GAL4 BD-SNARE fusions were grown in liquid selective media to OD600 = 1.0. Serial dilutions (total 10 μl) of cells were applied on agar plates lacking uracil and leucine (−URA/−LEU) for diploid growth, adenine (−ADE) for strong interaction, or histidine (−HIS) for weak interaction. Yeast diploids were scored for growth after 72 h at 30°C.

	COG1	COG2	COG3	COG4	COG5	COG6	COG7	COG8
BET1	–	–	–	–	–	–	–	–
GS15	–	–	–	–	–	–	–	–
GS27	–	–	–	–	–	A+/H+	–	A+/H+
GS28	–	–	–	–	–	–	–	–
SEC22	–	–	–	–	–	–	–	–
SNAP29	–	–	–	–	–	H+	–	–
STX5	–	–	–	A+/H+	–	A+/H+	–	A+/H+
STX6	–	–	–	–	–	A+/H+	–	H+
STX10	–	–	–	–	–	–	–	–
STX16	–	–	–	–	–	–	–	A+/H+
STX18	–	–	–	–	–	–	–	–
VAMP4	–	–	–	–	–	–	–	–
Vti1a	–	–	–	–	–	–	–	–
Vti1b	–	–	–	–	–	–	–	–
YKT6	–	–	–	–	–	–	–	–